

Multicomponent Physical Vapor Deposited Films with Homogeneous Molecular Material Distribution Featuring Improved Resist Sensitivity

Tristan Kolb, Christian Neuber, Marie Krysak, Christopher K. Ober, and Hans-Werner Schmidt*

Each film preparation technique affects the physical properties of the resulting coating and thus defines its applicability in modern device construction. In this context solvent based spin coated and solvent-free physical vapor deposited molecular glass photoresist films are systematically investigated for their dissolution behavior, sensitivity, and overall lithographic performance. These investigations demonstrate that the solvent-free physical vapor deposition leads to a marked increase in sensitivity. This could be explained by the individual molecule by molecule deposition step producing a more homogeneous distribution of the multicomponent resist system, especially the photoacid generator. In addition, this assumption is supported by former published simulations focusing on aggregate formation within thin films. This work demonstrates that the lithographic sensitivity of multicomponent resist system is an intrinsic parameter to investigate molecular material distribution and indicates that the applied film preparation technique is crucial for the corresponding performance and applicability.

1. Introduction

Thin films play an important role in current and emerging research fields, such as display technologies,^[1] solar cells,^[2] integrated circuits,^[3] SAMFETs,^[4] and data storage.^[5] In this context the application identifies the film preparation technique and thus the final quality and physical properties. The film processing can be classified as solvent based method, where the film forming materials are applied from solution, or as solvent-free method, where the materials are deposited out of a gas phase.^[6] The most prominent technique for solvent

based film processing is spin coating. Here, a solution is applied to a rotating substrate, which results in spreading and solvent evaporation. After a time period of several seconds up to a few minutes the solid material is typically obtained as a uniform, smooth film on the substrate.^[7] Advantages of spin coating are high reproducibility and uniform film formation on planar substrates up to diameters of more than 30 cm.^[8] Thereby film thicknesses from several nanometers up to millimeters are adjustable depending on solvent, concentration and viscosity of applied solution as well as acceleration to and adjusted final revolutions per minute of the spin coating process.^[9] Typically, investigated material classes range from inorganic materials to organic polymeric or low molecular weight materials.^[10–12]

However, there are requirements for the coating materials as sufficient solubility in non-corrosive or non-irritating solvents and suitable film forming properties. In some cases an alternative solvent-free film preparation technique can provide a remedy.^[13] Physical vapor deposition (PVD) is the most common method for solvent-free processing where the materials are evaporated or sublimed under high vacuum or/and a carrier gas. The resulting film is formed on a substrate by a molecule by molecule deposition during the PVD process. The controllable evaporation rate allows a precise film thickness control in the nanometer range monitored by quartz crystal microbalances. For the preparation of a multicomponent film the material composition is controlled by the individual evaporation rates of coevaporating components.^[14] The molecule by molecule coevaporation also results in a reduced molecular aggregation or segregation within the layer. The resulting film is pinhole-free and free from other impurities such as dust or solvent residues which can influence film formation and physical properties.^[15] However this method is only applicable for materials which can be evaporated or sublimed without thermal decomposition during the PVD process.

Due to the completely different film forming mechanisms of solvent based and dry preparation techniques, films produced can differ in crucial physical properties. This fact has been investigated in different research fields over the last five

T. Kolb, Dr. C. Neuber, Prof. H.-W. Schmidt
Macromolecular Chemistry I
Bayreuth Institute of Macromolecular Research (BIMF)
University of Bayreuth
95440 Bayreuth, Germany
E-mail: hans-werner.schmidt@uni-bayreuth.de
M. Krysak, Prof. C. K. Ober
Department of Materials Science
Cornell University
Ithaca, New York 14853, USA



DOI: 10.1002/adfm.201103130

years. In this context ultraviolet charged couple devices consisting of fluorescent pigment films showed differences upon annealing in the crystalline behavior in accordance with the film preparation technique.^[16] Bulk compounds compared to films prepared by PVD, spin coating or pulsed laser deposition (PLD) of chalcogenide glasses showed a huge impact on refraction index and optical bandgap.^[17] It was shown in detail that even related techniques such as PVD and PLD, both dry techniques differ only in the evaporation source utilizing thermal evaporation or pulsed laser ablation, can result in a change in microstructure causing an influence on the physical properties. Zirconium dioxide films as high refractive index material for optical coatings were also investigated by PVD and compared to a sol-gel spin coating process.^[18] The latter is a variation of the normal spin coating process where the solution contains precursors which form a gel-network by a condensation reaction in advance or even during the spin coating process. In this study differences in the absorption, the porosity ratio and the laser-induced damage threshold were demonstrated. For organic field-effect transistors the change of film application technique for pentacenes has been investigated for cost reduction. There the simpler process of the spin coating was applicable but has the drawback of decreased carrier mobility by one order of magnitude.^[19]

For two or more component systems in addition the miscibility and blending of these different components has to be considered. Segregation or phase separation can interfere with homogeneous material distribution.^[20,21] The resulting film is not only affected by the miscibility of the materials but also by the preparation technique. This places for example importance on processing in organic light emitting devices (OLED), where the phosphorescence emitter has to be applied in a quantity that avoids concentration quenching.^[22] For this purpose the devices are usually prepared by PVD,^[23] which ensures by the molecule by molecule deposition that a statistically controlled homogenous material distribution is produced. In addition this technique allows the fabrication of the established multilayer devices.

A homogeneous material distribution is also considered as an issue in lithography. State of the art multicomponent chemically amplified photoresist systems are successful due to their high sensitivity.^[24] For this purpose photoresist systems consist of at least a photoacid generator (PAG) and an acid sensitive matrix compound. During exposure the PAG has to be activated to release an acid, which catalyzes in the subsequent post exposure bake (PEB) deprotection or crosslinking reactions in the matrix compound resulting in the solubility contrast. An irregular distribution of PAG is assumed to contribute to the problem of line edge roughness.^[25] Due to this relevance the material distribution in small domains was studied by NMR techniques for similar systems.^[26,27] However by this method no proof of molecular blending was possible at small dimensions for materials having good miscibility but systems of poor miscibility showed phase separation. Unfortunately, only bulk samples were investigated, whose properties can differ from thin films and their application in lithography. A theoretical study of the influences of PAG distribution - smaller versus bigger aggregates - was investigated by two-dimensional Monte Carlo simulations.^[28] These demonstrate that depending on the

diffusion length, the resist performance characterized by resolution, line edge roughness (LER) and sensitivity was affected by the PAG matrix blending. This result concerning LER was also confirmed in three-dimensional simulations.^[29] Consequently differences in blending caused by the applied film preparation technique should result in performance distinctions in sensitivity and the overall pattern quality.

In the literature there are some recent publications on solvent-free resist film preparation by PVD.^[30,31] However this technique places demands on the resist systems concerning the evaporability of the components. For this purpose a molecular glass resist^[32] must be applied instead of the typical commercial polymeric matrix materials and the standard ionic PAGs have to be replaced by nonionic ones.

In this work we investigated a molecular glass negative resist consisting of a phenolic matrix, a crosslinker and a PAG focusing performance distinctions originating from the applied film preparation technique. We investigated the dissolution behavior, the sensitivity and the overall performance in lithographic patterning of films prepared by the solvent-based process of spin coating and compared it to the solvent-free PVD process. Due to molecular deposition in PVD the three components should be well distributed without aggregate formation while for spin coating the evaporation of the often utilized polar solvent can result in directional transport of the polar photoacid generator (PAG) to the film surface.^[20] Furthermore the molecular nature and size of the constituents in the latter case, enable aggregate formation during solvent evaporation and film formation, which should affect lithographic performance (Figure 1).

2. Results and Discussion

2.1. The Lithographic Process and Identified Process Variables

The investigation of differences in the lithographic performance originating from different film preparation techniques requires the identification of several key variables. The lithographic process (Figure 2) starts typically with the film preparation step on a primed Si-wafer. For the work presented two different film preparation techniques were investigated. For this purpose a molecular glass photoresist, composed of a phenolic matrix, a crosslinker and a PAG, was applied by both spin coating and physical vapor deposition (PVD). In the case of the solvent cast films a post application bake (PAB) step to remove any remaining solvent was used. For the film preparation by the solvent-free PVD process this step is unnecessary and consequently was not applied. Afterwards the film was exposed to either UV radiation (240 nm to 290 nm) or an electron beam to expose the PAG. The resulting acid catalyzes the crosslinking reaction during the post exposure bake step resulting in the dissolution contrast between exposed and unexposed areas. Finally after development, with appropriate developer and development time, the final patterns were achieved.

Two strategies were identified to investigate possible process variables influencing the resist performance depending on the applied film preparation technique. The final patterns were

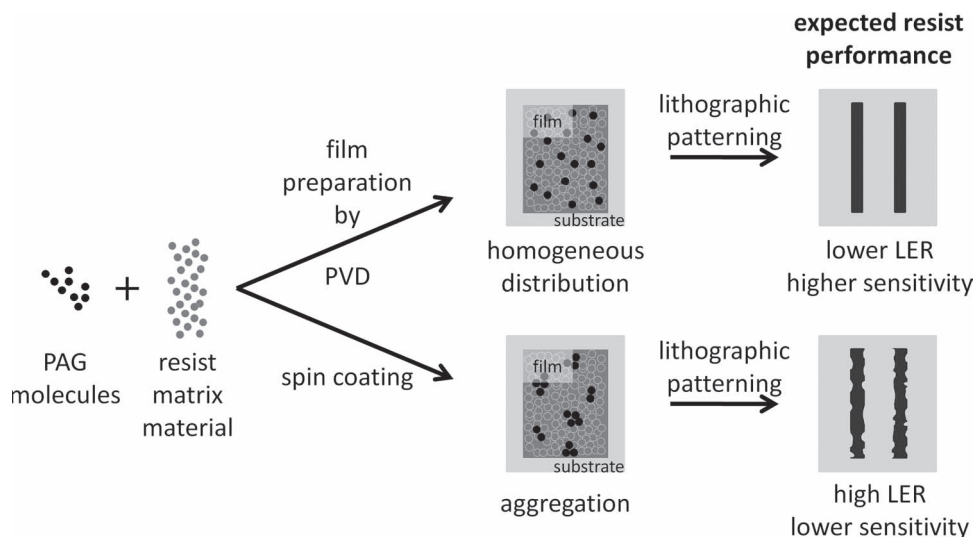


Figure 1. Schematic illustration of expected resist performance originating from the film preparation technique by the different given PAG distribution in a chemical amplified photoresist.

evaluated with respect to pattern performance. In addition changes in the photoresist characteristics like sensitivity or dissolution behavior are directly measurable.

2.2. Dissolution Investigations

The knowledge about the dissolution behavior of a photoresist system is crucial for selecting appropriate development conditions. For efficient lithographic patterning the dissolution

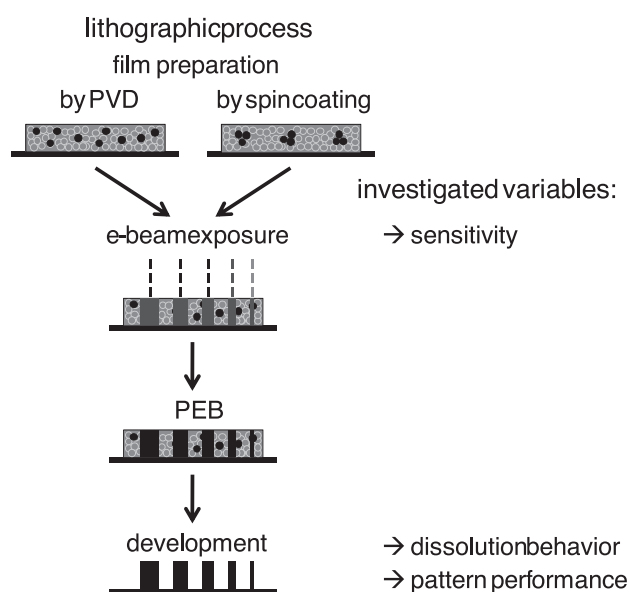


Figure 2. Schematic of the lithographic process of investigated negative molecular glass resist with film preparation, exposure, post exposure bake (PEB), and pattern development. In addition the variables of the processing steps are allocated, which were investigated for solvent-free or solvent-based prepared resist films.

contrast resulting from exposure and thermal treatment obtained between exposed and unexposed resist zones defines the patternability itself and its performance. In this context the applied film preparations technique and thus the resulting intrinsic film properties such as density, smoothness, and uniformity of material blending should affect the dissolution behavior. Our dissolution investigations deal with unexposed and fully crosslinked resist films on a quartz crystal microbalance (QCM) representing both material states before and after lithographic patterning. The measurement principle is based on the monitoring of the oscillation damping of quartz crystals (QC's) resulting from deposited material on the surface.^[33] For this work films were applied onto QC's by PVD as well as by spin coating. After PAB for the spin coated sample a flat exposure with UV-light (240 nm to 290 nm) was performed on two different prepared films with a dose of 246 mJ cm^{-2} . This high dose guaranteed a high photo activation ratio of the PAG and thus a high conversion of crosslinking during the PEB process step at elevated temperatures of 95°C . In this way QCs with crosslinked films and with unexposed native photoresist materials prepared by the solvent-free and solvent based techniques were available for the dissolution investigations.

The finished QC's were fixed into the QC-holder, the monitoring of the oscillation frequency was started, and the corresponding QC placed into a beaker containing at the beginning stirred deionized water. During monitoring developer strength was increased in several concentration steps so the dissolution behavior was studied over a wide concentration range of tetramethylammonium hydroxide (TMAH) solutions.

In **Figure 3** the resulting dissolution graphs are presented for spin coated and PVD prepared films in the unexposed and exposed state. The unexposed material shows for the solution coated as well as for the PVD prepared film a nearly identical behavior and thus no dissolution differences originated from the film preparation technique was measured by the QCM measurement. Their measured dissolution behaviors show a

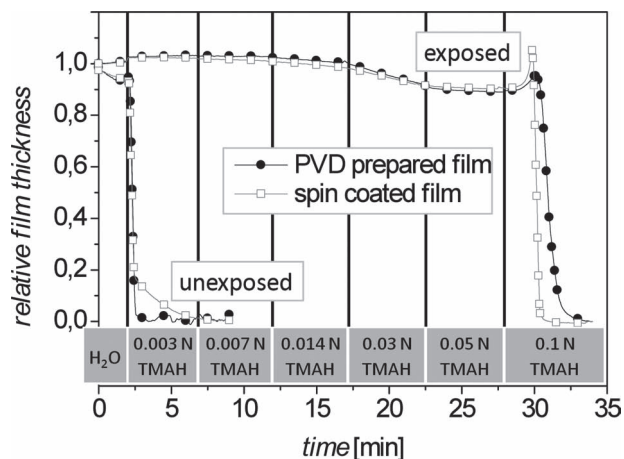


Figure 3. Dissolution behavior investigation of solution and PVD prepared films by quartz crystal microbalance measurements; unexposed and exposed films (UV exposure: 240 nm to 290 nm, 246 mJ cm^{-2} , PEB 30 s at 95 °C) were dipped into pure water at the beginning. Then after defined time periods small amounts of tetramethylammonium hydroxide (TMAH) were added resulting in a stepwise increase of developer strength.

slight decrease in film thickness in pure water explainable by the modest solubility of the unexposed resist material. After the addition of a small amount of TMAH, resulting in a 0.003 N solution, the unexposed resist material dissolves spontaneously. The films exposed to UV light and then thermally annealed showed in comparison to the unexposed a dissolution contrast. However, again a nearly identical dissolution behavior was measured independent of the applied film preparation technique. Here the QCM calculated film thickness is nearly constant up to a 0.007 N TMAH concentration, decreases slightly between the TMAH concentrations of 0.014 N to 0.05 N, and drops remarkably at the TMAH concentration of 0.1 N after a short swelling period. In conclusion this measurement demonstrates that at a 0.1 N TMAH concentration even the exposed negative type resist and thus the patterns are stripped off. For this reason the development step for the following experiments were performed with 0.05 N TMAH meaning working at the highest acceptable contrast between unexposed and exposed resist material. By this investigation it was also shown that independent from the applied film preparation technique the photoresist films have the same measured dissolution characteristics, as a consequence there are no measureable dissolution differences or the QCM measurement is unable to detect slight discrepancies. But this sensitive technique demonstrates in combination with a stepwise increase of the developer strength a powerful tool for measuring crucial dissolution characteristics of film materials, here to quantify the dissolution contrast.

2.3. Resist Sensitivity

In the following section the lithographic sensitivity of films prepared by either spin coating or PVD were investigated. For this purpose the standard technique for measuring a lithographic

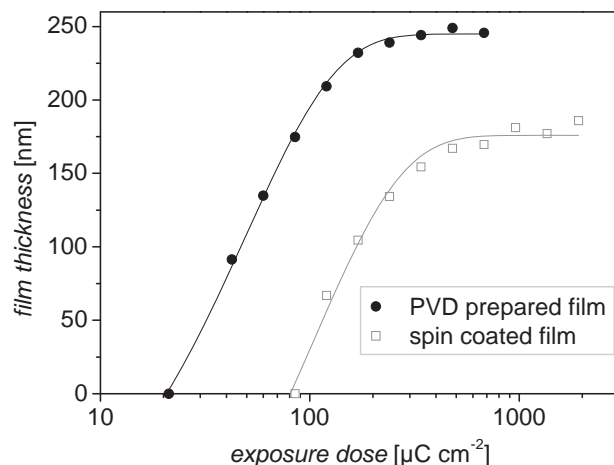


Figure 4. Contrast curves of resist films prepared by spin coating (gray open squares) and physical vapor deposition (black closed circles) with the applied fit (gray and black lines, Equation 1). The PVD prepared film shows a significant increase in sensitivity while the contrast of the resist remains approximately the same.

contrast curve^[32] was applied by utilizing an electron beam (ebeam) exposure tool. Therefore the two film types were exposed to multiple squares of different doses by ebeam and after PEB developed. The resulting pattern height of the different squares was measured by a stylus profiler. In **Figure 4** the contrast curves, hence the dose dependence of the measured square heights in nm, for the by PVD and by spin coating prepared films are shown.

The graphs show that both films have nearly the same resist contrast, defined by the slope of the contrast curve. This is as expected due to the fact that this value is material composition dependent which is the same for both preparation methods. However a clear difference in sensitivity is observed for the different prepared films whereas all other lithographic processing steps and conditions were applied identically. Keeping in mind the results of the already mentioned theoretical simulation^[28] this experiment indicates that the two investigated film preparation techniques, PVD and spin coating, have different blending capabilities. The PVD technique provides obvious advantages due to its single molecule by molecule deposition of a well distributed mixture of the three components through the complete resist film. In contrast the solvent based spin coating process produces resist films of lower sensitivity and this fact can be explained by possible PAG aggregate formation. Mack et al.^[34] (**Table 1**) introduced a way to calculate significant values in terms to sensitivity based on the experimental data of the measured film thickness T_r at the correspondingly applied exposure dose E by fitting the graphs with Equation 1.

$$T_r = T_0 - \Delta T_{\max} e^{-E/E_n} \quad (1)$$

Herein describes T_0 the native resist film thickness, while ΔT_{\max} represents the theoretical value of the maximal crosslinkable resist thickness and E_n a sensitivity term for negative type resists. By applying these fitting parameters to Equation 2, also introduced by Mack et al.^[34] the gel dose E_0 can be calculated.

Table 1. Significant values in terms to sensitivity of the fitted contrast curves (Figure 4) and out of this calculated gel dose E_0 for a quantitative sensitivity investigation of films prepared by spin coating or PVD.

	$T_0^a)$ [nm]	$\Delta T_{\max}^b)$ [nm]	$E_n^c)$ [$\mu\text{C cm}^{-2}$]	E_0 [$\mu\text{C cm}^{-2}$]
Spin coating	175.9	386.1	102.6	80.6
PVD	244.9	347.0	51.3	17.9

^{a)}Native resist film thickness; ^{b)}Maximal crosslinkable resist thickness; ^{c)}Sensitivity term for negative resists.

This value characterizes the theoretical dose where first material remains after development in the exposed areas.

$$E_0 = -E \ln \left(\frac{T_0}{\Delta T_{\max}} \right) \quad (2)$$

Applying the equations to the investigated PVD prepared resist films a four time increase in sensitivity quantified by the gel dose E_0 and a two time increase in sensitivity term E_n in comparison to spin coated samples were achieved. In conclusion lithographic contrast curves of an identical patterned resist system are highly sensitive to the applied film preparation technique and this indicates a different blending of photo acid generator within the resist material.

2.4. Resist Performance

In addition to the sensitivity the general resist performance and its dependence on the film preparation technique was investigated. Therefore the applied processing variables of the delicate lithographic process to the solvent-free and solvent based films were optimized individually. This issue is addressed in this work by the systematic variation of the important processing variables of exposure dose, PEB temperature and development conditions. Due to the fact that all of these variables depend on each other, this variation is realized in one experiment by gradients in a combinatorial library. The prepared combinatorial libraries based on PVD prepared or spin coated films allowed a fast and efficient observation of the overall best performance of the patterns identified in defined sectors. A schematic figure of the arrangement of the investigated variable gradients in the combinatorial library is shown in **Figure 5**.

For the ebeam exposure the defined sectors are arranged in a grid of 4 columns and 6 rows on the substrate. In addition, every sector consists of 22 rows with 100 nm lines (1/1 and 1/2 line space pattern). Each exposure row is exposed with a different dose resulting in the exposure dose gradient ranging from $9 \mu\text{C cm}^{-2}$ to $414 \mu\text{C cm}^{-2}$. The exposed substrate with the 24 sectors was afterwards subjected to the horizontal PEB temperature gradient ranging from 89°C to 63°C . This thermal treatment enables the acid catalyzed crosslinking of the resist material. For the development step a time gradient between 8 s and 181 s was arranged orthogonal to the applied temperature gradient. By applying these three gradients very similar combinatorial libraries for the spin coated and the PVD prepared films were available. **Figure 6a** shows the SEM image of solution cast

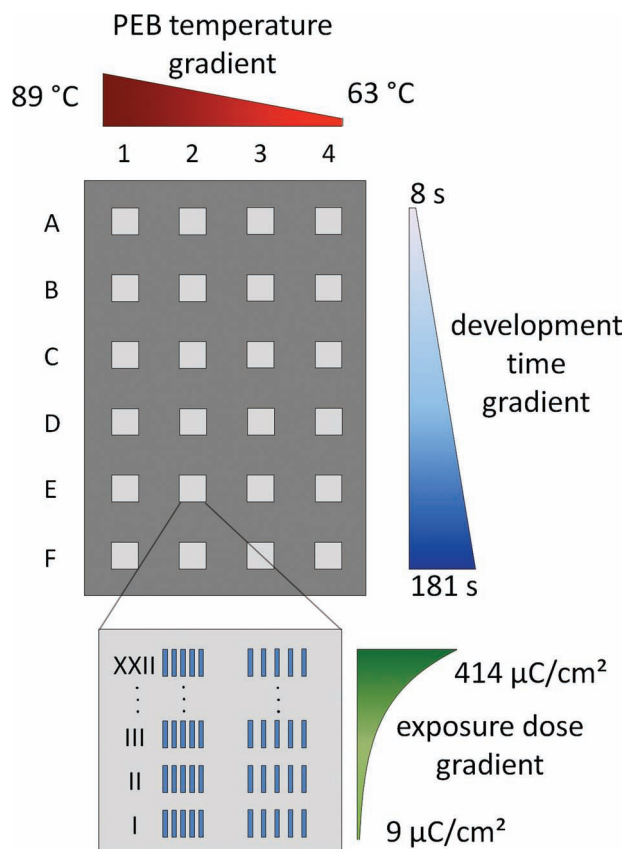
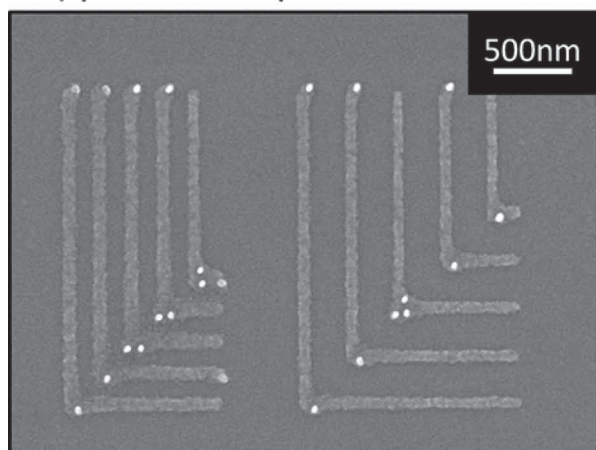


Figure 5. Schematic illustration of the investigated combinatorial library for the optimization of exposure dose, PEB temperature, and development time in one experiment. The combinatorial library consists of a horizontal PEB temperature gradient ranging from 89°C to 63°C , a vertically development time gradient of 8 s to 181 s and an exposure dose gradient ranging from $9 \mu\text{C cm}^{-2}$ to $414 \mu\text{C cm}^{-2}$ applied in each sector.

combinatorial optimized 100 nm L-shaped line pattern. Due to the lack of additional scientific information of the L-shaped pattern we simplified the pattern for the following lithographic investigations and observed the 100 nm simple line pattern obtained by utilizing a physical vapor deposited film applying the same resist composition (Figure 6b).

The best pattern of the solution cast film was observed at an exposure dose of $96 \mu\text{C cm}^{-2}$ (dose XIV) in sector B2 corresponding to a PEB at 80°C and development time of 43 s in stirred 0.05 N TMAH solution. The pattern is obviously well developed and shows clear lines. For the evaporated film the best pattern was observed at the lower dose of $58 \mu\text{C cm}^{-2}$ (dose XI) in sector D2 corresponding to a PEB at 80°C and development of 113 s in stirred 0.05 N TMAH solution. In contrast to the solution prepared film the pattern of the PVD prepared film shows residual material around the distinct lines and primarily between the lines even at the clear lower exposure dose and the drastic elongation of development time period. The observation, that these residues are only observable in the vicinity of pattern and that they cannot be removed even under enhanced developing conditions, indicates the presence of crosslinked photoresist materials activated by backscattered electrons. In

a) pattern of spin coated film



b) pattern of PVD prepared film

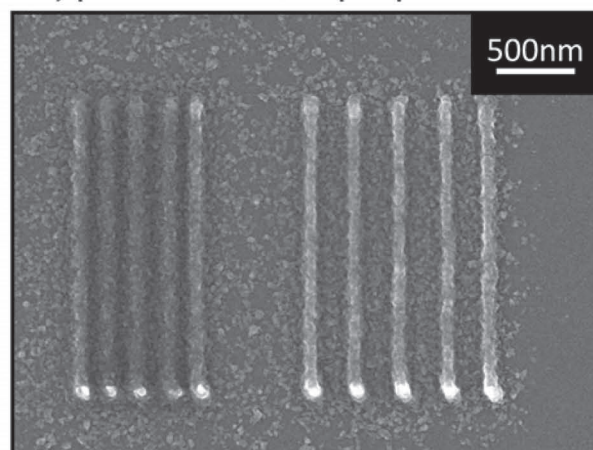


Figure 6. SEM images of patterns taken from the optimized sectors of the combinatorial library based on solution cast and physical vapor deposited films. a) Spin coated: pattern of sector B2 was observed at a PEB of 80 °C, a development time of 43 s and an exposure dose of 96 $\mu\text{C cm}^{-2}$. The features are well developed and show clear lines. b) PVD prepared: pattern of sector D2 was observed at a PEB of 80 °C, a development time of 113 s and an exposure dose of 58 $\mu\text{C cm}^{-2}$. The pattern shows residual material around the distinct lines. These residues are caused by backscattered electrons due to the increased sensitivity of PVD prepared films.

conclusion these observations and the applied lower ebeam dose demonstrate a crucial increased sensitivity of the same resist system utilizing PVD as film preparation technique.

2.5. Optimization of Resist Performance

It is known that an increased acceleration voltage of an ebeam tool reduces the local dose originating from backscattered electrons due to an increased penetration depth.^[35] Therefore further patterning experiments for PVD prepared resists were performed at a 100 kV professional ebeam tool. In addition sensitivity screening investigations on eight different PAGs identified 2-[(methylsulfonyl)oxy]-1H-benz[de]isoquinoline-1,3(2H)-dione (PAG2) as the most sensitive non-ionic ebeam photo acid generator and thus it was applied for the following patterning experiments. Again a combinatorial library as shown in Figure 5 was prepared based on a PVD prepared film for the optimization of exposure dose, PEB temperature and development conditions. Here, for ebeam exposure several sectors were arranged in a grid of 25 columns and 3 rows where each sector consists of 24 dose arrays. Each dose array was exposed with a dose range from 24 $\mu\text{C cm}^{-2}$ to 215 $\mu\text{C cm}^{-2}$ defining the exposure dose gradient. The exposed substrate was then annealed by a PEB temperature gradient between 105 °C and 77 °C. For development a time step gradient of 10 s, 20 s and 30 s in the orthogonal direction to the PEB temperature gradient was applied. The overall best pattern on the whole substrate concerning lack of residue formation and blur is shown in Figure 7. The SEM image shows compact lines with some remaining residues, but in comparison to the result achieved with a 20 kV ebeam tool a reduction of residue formation was observable just as a result of the exchange of PAG and the utilization of a higher acceleration voltage.

In addition, for overcoming the issue of residue formation due to backscattering an extra bottom buffer layer between the substrate and the resist film was applied. Such an intermediate layer reduces the amount of backscattered electrons arriving the resist layer due to an increased distance between silicon wafer and resist film. An important requirement for such a bottom buffer layer is the atomic composition of only low average atomic number resulting in very little contribution to the amount of scattered electrons. In screening experiments poly-2-vinylpyridine (P2VP), polymethylmethacrylate

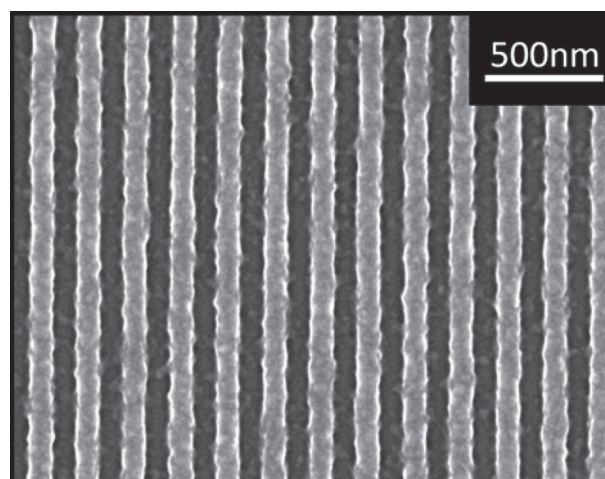


Figure 7. SEM image of the pattern observed on the optimized sectors of the combinatorial library of PVD prepared resists patterned with a 100 kV ebeam tool. Lines were observed at a PEB of 99 °C, a development time of 10 s, and an exposure dose of 75 $\mu\text{C cm}^{-2}$ at 100 kV. The features showed compact lines with some residues in between.

(PMMA) and crosslinked resist films consisting of Trisphenol, Powderlink and triphenylsulfonium perfluorobutanesulfonate were investigated. First each of these materials was coated on silicon substrates of a 100 nm final film thickness. Then on top of each buffer layer a 100 nm thick resist film was prepared by PVD. The UV crosslinked resist buffer layer showed weak performance presumably due to remaining active acid within the layer. This acid diffuses during PEB into the vapor deposited resist film resulting in residue formation. With PMMA as bottom buffer layer no features could be observed due to stripping during the development process. Within screening the P2VP bottom buffer layer showed the best performance with reduced residue formation. However, P2VP shows dissolution in the organic solvent used for spin-coating. Also no alternative orthogonal application solvent was found. Thus, it was impossible to prepare solution cast resist films on the bottom buffer layer. Therefore, P2VP was only investigated for the PVD prepared resist and thus applied in an additional combinatorial patterning experiment as bottom buffer layer. Therefore a similar combinatorial library as described above for the optimization of exposure dose, PEB temperature and development conditions was applied to a resist film prepared by PVD on a silicon wafer coated with a 100 nm thick layer of P2VP as bottom buffer layer. Again several sectors were arranged in a grid of 25 columns and 3 rows where each sector consists of 24 dose arrays. Each dose array was exposed with a dose range from $24 \mu\text{C cm}^{-2}$ to $215 \mu\text{C cm}^{-2}$ defining the exposure dose gradient. After this the exposed substrate was then annealed by a PEB temperature gradient between 105°C and 77°C . For development a time step gradient of 10 s, 20 s, and 30 s in the orthogonal direction to the PEB temperature gradient was applied. The overall best pattern on the whole substrate concerning lack of residue formation and blur is shown in **Figure 8**.

The patterning of the resist film on the P2VP bottom buffer layer was achieved with the resist composition of 78.4 wt%

phenolic matrix, 19.3 wt% crosslinker and only 2.3 wt% PAG2 at a PEB temperature of 105°C , a development time of 20 s and an exposure dose of only $26.4 \mu\text{C cm}^{-2}$. The observed clear lines demonstrate that the introduction of the bottom buffer layer P2VP has no impact to the high sensitivity of this PVD resist but successfully suppresses the residue formation due to backscattered electrons. Unfortunately, the lines are not perfectly parallel, a sign for weak anchoring of the exposed resist to the bottom buffer layer interface. Thus in further studies additional bottom buffer layer materials will be screened to manipulate or optimize further the interface properties. However, this work demonstrates the successful concept of reducing the impact of backscattered electrons and achieving clear 100 nm patterns by introducing an organic bottom buffer layer between a high sensitive resist material and the silicon substrate.

3. Conclusions

In this work the resist performance of films prepared by different film preparation techniques, solution based spin coating and solvent-free physical vapor deposition (PVD), were investigated for the first time. Their dissolution behaviors were examined by applying the quartz crystal microbalance technique in combination with a stepwise increase of the developer strength, allowing quantification of the development contrast. Sensitivity measurements by contrast curve investigations show a crucial increase in sensitivity of solvent-free prepared resist films in comparison to the solvent-based resist film. The increased sensitivity is explained by the more homogeneous material distribution given by the molecular PVD process. The optimization of the delicate lithographic process variables in view to performance was performed efficiently by ternary combinatorial libraries of exposure dose, post exposure bake temperature and development time. This experiment confirmed the sensitivity increase by utilizing PVD as film preparation technique and thus demonstrates in agreement with theoretical predictions the importance of a homogeneous PAG distribution in chemical amplified resist systems. Unfortunately, the increased sensitivity effects the formation of residues originated from backscattered electrons. But utilizing a 100 kV ebeam tool and applying a bottom buffer layer clear 100 nm pattern of the high sensitive PVD prepared resist film are observed. In conclusion this work demonstrates that applying PVD as solvent-free film preparation technique improves the overall resist performance by optimizing the intrinsic film properties influenced by e.g. the material blending and remaining solvent.

4. Experimental Section

Film Preparation by Physical Vapor Deposition and Spin Coating: The investigated photoresist system consisted of the phenolic matrix 1,1,1-tris(4-hydroxyphenyl)-1-ethyl-4-isopropylbenzene (purchased from ABCR), the crosslinker N,N',N'',N'''-tetra(methoxymethyl)glycoluril (purchased from Worlée-Chemie) and the photoacid generator (PAG1) 1,2,3-tris(methanesulfonyloxy)benzene (purchased from Midori Kagaku). For the film preparation by physical vapor deposition (PVD) these components were coevaporated by utilizing three effusion cells where the respective evaporation rate is adjusted by heating and

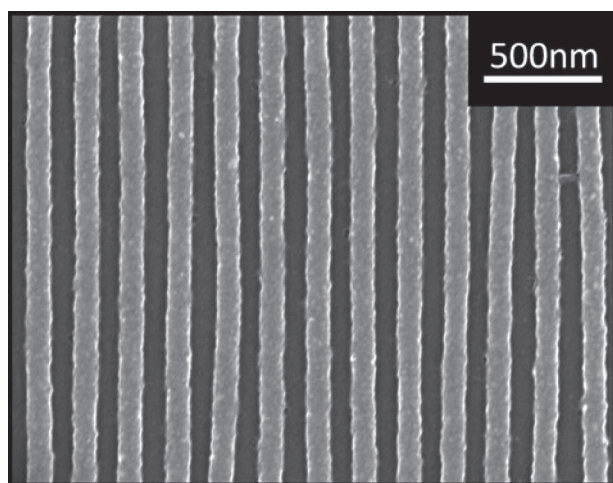


Figure 8. SEM images of pattern observed at the optimized sectors of the combinatorial library of PVD prepared resists with an extra applied bottom buffer layer. Lines were observed at a PEB of 105°C , a development time of 20 s, and an exposure dose of $26.4 \mu\text{C cm}^{-2}$. No residues are observable.

monitored by a quartz crystal microbalance (QCM).^[14] The overall film deposition rate ($\sim 1 \text{ Å s}^{-1}$) and thus the film thickness are controlled by two additional QCMs just beside the rotating substrate. To achieve an efficient adsorption of the evaporating molecules the substrate is cooled by a Peltier element to 10°C . For the investigation of the dissolution properties 1 inch 5 MHz quartz crystals (QC) with polished gold surface (purchased from Inficon) and 4 inch Hexamethyldisilazane (electronic grade, purchased from ABCR) primed silicon wafers (n-doped, crystal orientation (100), purchased from Crystec) for the remaining experiments were utilized. The exact evaporated compositions (76 wt% phenolic matrix, 19 wt% crosslinker and 5 wt% PAG1 for the dissolution investigations respectively 79 wt% phenolic matrix, 16 wt% crosslinker and 5 wt% PAG1 for the other experiments) were measured by high performance liquid chromatography (HPLC).

Comparable spin coated films were prepared from solutions with the same ratios as of the PVD prepared films of the photoresist components in propylene glycol monomethyl ether acetate (PGMEA, purchased from Aldrich). After spin coating on QC respectively primed silicon wafers a post application bake (PAB) for 30 s at 115°C was performed with the object of solvent removal and thermal relaxation of film material.

For subsequent patterning experiments with a 100 kV ebeam tool films with the more sensitive photoacid generator 2-[(methylsulfonyl)-oxy]-1H-benz[de]isoquinoline-1,3(2H)-dione (PAG2, purchased from Midori Kagaku) were prepared by PVD on substrates primed with HMDS respectively coated with a 100 nm thick layer of poly-2-vinylpyridine (P2VP). By HPLC again the composition were determined for the film on the HMDS primed substrate (75.9 wt% phenolic matrix, 22.8 wt% crosslinker and 1.3 wt% PAG2) as well as for the film on the P2VP coated substrate (78.4 wt% phenolic matrix, 19.3 wt% crosslinker and 2.3 wt% PAG2).

Dissolution Investigations: The investigation of the dissolution process is based on the monitoring of the resonance frequency of QC, whose frequency shift during application or removal of film material on QC surface is proportional to its mass respectively its film thickness.^[36] Thus this technique allows a sensitive monitoring of dissolution or swelling processes. For this study 50 nm thick films were prepared by PVD as well as by spin coating on QC and were investigated unexposed and exposed (crosslinked). For the latter the films on the QCs were flood exposed to UV light (240 nm–290 nm) with a dose of 246 mJ cm^{-2} and then applied to a post exposure bake (PEB) of 95°C for 30 s yielding crosslinked films. Afterwards the exposed and unexposed samples are mounted in the QC-holder (Maxtec CHC-100) and the assembled working QCM immersed into stirred deionized water. Thus the recorded frequency shows the dissolution behavior of corresponding films in deionized water. By adding small amounts of concentrated tetramethylammonium hydroxide solution (TMAH) a stepwise increase in developer concentration was realized. This allowed the systematical study of the dissolution behavior of the photoresist films over a spectrum of different development conditions in one experiment.

Sensitivity Investigations: For the investigation of the ebeam sensitivity the standard procedure for measuring a contrast curve was applied.^[32] For this purpose 100 nm thick films are prepared by spin coating and by PVD on silicon wafers, afterwards exposed with multiple squares of different doses with an acceleration voltage of 20 kV at a Zeiss LEO 1530 equipped with a Raith Elphy Plus and after post exposure bake (30 s; 80°C) developed (20 s; 0.05 N TMAH). The obtained film height of the squares resulting from the different applied doses was measured by a stylus profiler (Veeco Dektak 150).

Patterning Process: 100 nm thick photoresist films prepared on silicon wafer by spin coating or PVD were patterned utilizing a combinatorial approach. This allowed the variation of important processing variables in one experiment to identify influences resulting from the different film preparation techniques. For this purpose in a combinatorial library gradients of the processing variables exposure dose, PEB temperature and development time were arranged. The exposure was carried out with an acceleration voltage of 20 kV at a Zeiss LEO 1530 equipped with a Raith Elphy Plus in 24 separate write fields ($51.2 \mu\text{m} \times 51.2 \mu\text{m}$) arranged in a grid of 4 columns and 6 rows. Each write field consists

of 22 similar 100 nm line/space patterns exposed to different doses, between $9 \mu\text{C cm}^{-2}$ and $414 \mu\text{C cm}^{-2}$. The temperature gradient for PEB is realized on a stainless steel plate by active cooling with liquid nitrogen on the one side and heating up to 300°C by a hot plate on the other side. By an infrared camera the establishment of the equilibrated temperature gradient is monitored and the achieved temperatures are measured on a reference silicon wafer. The exposed film is placed for 30 s just beside the reference wafer in the desired temperature range resulting in a PEB temperature gradient for column 1 to 4 between 89°C and 63°C . The continuous development time gradient between 8 s and 181 s for row A to F in orthogonal direction to the PEB temperature gradient is realized by immersion of the substrate with a motor drive into the development bath containing stirred 0.05 N TMAH. After sputtering the sample with platinum the combinatorial library was evaluated by SEM regarding the different sectors and the applied exposure doses. The overall best pattern represents the optimized conditions for the combinatorial optimized variables.

For subsequent experiments with the aim of residue reduction 100 nm thick resist films were prepared by PVD on silicon substrates coated with 100 nm of poly-2-vinylpyridine (P2VP) as a bottom buffer layer as well as just primed silicon substrates for comparison. On both substrates a similar combinatorial library as before were arranged but this time exposed with a JOEL JBX-9300FS 100 kV ebeam tool with applied proximity correction. The exposure was carried out in 75 separate write fields arranged in a grid of 25 columns and 3 rows. Each write field features 96 nm line/space patterns and includes a dose array of 24 different doses ranging between $24 \mu\text{C cm}^{-2}$ and $215 \mu\text{C cm}^{-2}$ yielding an exposure dose gradient. Afterwards the exposed substrates were subject to a PEB temperature gradient between 105°C and 77°C for 30 s. For development in 0.05 N TMAH a development time step gradient of 10 s, 20 s and 30 s in orthogonal direction to the PEB temperature gradient was applied. After sputtering the sample with platinum the combinatorial library was evaluated by SEM regarding the different sectors and the applied exposure doses. The overall best pattern on the whole substrate concerning lack of residue formation and blur mirrors the optimized values of these variables in regard to the others.

Acknowledgements

This work was supported by the Semiconductor Research Corporation's Global Research Collaboration (GRC) Program (Task 1675.001), the German Research Foundation (Deutsche Forschungsgemeinschaft), Collaborative Research Center (Sonderforschungsbereich) 481, project A6, and Elite Network of Bavaria. This work was performed in part at the Cornell NanoScale Facility, a member of the National Nanotechnology Infrastructure Network, which is supported by the National Science Foundation (Grant ECS-0335765).

Received: December 24, 2011

Revised: May 2, 2012

Published online: May 25, 2012

- [1] B. Geffroy, P. Le Roy, C. Prat, *Polym. Int.* **2006**, *55*, 572.
- [2] Y. Ma, Y. Wen, Y. Song, *J. Mater. Chem.* **2011**, *21*, 3522.
- [3] International Technology Roadmap for Semiconductors (ITRS) **2011**, www.itrs.net (accessed May 2012).
- [4] B. C. Popere, A. M. Della Pelle, A. Poe, S. Thayumanavan, *Phys. Chem. Chem. Phys.* **2012**, *14*, 4043.
- [5] E. C. P. Smits, S. G. J. Mathijssen, P. A. van Hal, S. Setayesh, T. C. T. Geuns, K. A. H. A. Mutsaers, E. Cantatore, H. J. Wondergem, O. Werzer, R. Resel, M. Kemerink, S. Kirchmeyer, A. M. Muzafarov, S. A. Ponomarenko, B. de Boer, P. W. M. Blom, D. M. de Leeuw, *Nature* **2008**, *455*, 956.

- [6] T. Shimoda, Y. Matsuki, M. Furusawa, T. Aoki, I. Yudasaka, H. Tanaka, H. Iwasawa, D. Wang, M. Miyasaka, Y. Takeuchi, *Nature* **2006**, *440*, 783.
- [7] K. Norrman, A. Ghanbari-Siahkali, N. B. Larsen, *Annu. Rep. Prog. Chem., Sect. C: Phys. Chem.* **2005**, *101*, 174.
- [8] J.-Y. Jung, Y.-T. Kang, J. Koo, *Int. J. Heat Mass Transfer* **2010**, *53*, 1712.
- [9] D. W. Schubert, T. Dunkel, *Mater. Res. Innovations* **2003**, *7*, 314.
- [10] N.-H. Kim, P.-J. Ko, W.-S. Lee, *J. Vac. Sci. Technol. A* **2008**, *26*, 794.
- [11] T. Leveder, S. Landis, N. Chaix, L. Davoust, *J. Vac. Sci. Technol. B* **2010**, *28*, 1251.
- [12] S. Tang, M. Liu, P. Lu, H. Xia, M. Li, Z. Xie, F. Shen, C. Gu, H. Wang, B. Yang, Y. Ma, *Adv. Funct. Mater.* **2007**, *17*, 2869.
- [13] S. M. Rosnagel, *J. Vac. Sci. Technol. A* **2003**, *21*, S74–S87.
- [14] C. Neuber, M. Bate, M. Thelakkat, H.-W. Schmidt, H. Hansel, H. Zettl, G. Krausch, *Rev. Sci. Instrum.* **2007**, *78*, 72216.
- [15] C. A. Mack, *Fundamental principles of optical lithography: The science of microfabrication*, John Wiley & Sons Ltd, Chichester, England **2007**, Ch. 5.
- [16] S. J. Keough, T. L. Hanley, A. B. Wedding, J. S. Quinton, *Surf. Sci.* **2007**, *601*, 5744.
- [17] M. Krbal, T. Wagner, T. Kohoutek, P. Nemec, J. Orava, M. Frumar, *J. Phys. Chem. Solids* **2007**, *68*, 953.
- [18] Y. J. Guo, X. T. Zu, X. D. Jiang, X. D. Yuan, S. Z. Xu, B. Y. Wang, D. B. Tian, *Opt. Laser Technol.* **2008**, *40*, 677.
- [19] X. Wang, S. Ochiai, K. Kojima, A. Ohashi, T. Mizutani, *J. Vac. Soc. Jpn.* **2008**, *51*, 169.
- [20] E. L. Jablonski, V. M. Prabhu, S. Sambasivan, D. A. Fischer, E. K. Lin, D. L. Goldfarb, M. Angelopoulos, H. Ito, *Proc. SPIE* **2004**, *5376*, 302.
- [21] T. Xu, H.-C. Kim, J. DeRouche, C. Seney, C. Levesque, P. Martin, C. M. Stafford, T. P. Russell, *Polymer* **2001**, *42*, 9091.
- [22] M. A. Baldo, S. Lamansky, P. E. Burrows, M. E. Thompson, S. R. Forrest, *Appl. Phys. Lett.* **1999**, *75*, 4.
- [23] K. Kreger, M. Baete, C. Neuber, H.-W. Schmidt, P. Strohrriegel, *Adv. Funct. Mater.* **2007**, *17*, 3456.
- [24] H. Ito, *Adv. Polym. Sci.* **2005**, *172*, 37.
- [25] T. Hirayama, D. Shiono, S. Matsumaru, T. Ogata, H. Hada, J. Onodera, T. Arai, T. Sakamizu, A. Yamaguchi, H. Shiraishi, H. Fukuda, M. Ueda, *Proc. SPIE* **2005**, *5753*, 738.
- [26] S. J. Limb, B. E. Scruggs, K. K. Gleason, *Macromolecules* **1993**, *26*, 3750.
- [27] D. L. VanderHart, V. M. Prabhu, E. K. Lin, *Chem. Mater.* **2004**, *16*, 3074.
- [28] R. A. Lawson, C. L. Henderson, *Proc. SPIE* **2009**, *7273*, 727341/1.
- [29] T. Kozawa, H. Yamamoto, S. Tagawa, *J. Photopolym. Sci. Technol.* **2010**, *23*, 625.
- [30] F. Pfeiffer, N. M. Felix, C. Neuber, C. K. Ober, H.-W. Schmidt, *Adv. Funct. Mater.* **2007**, *17*, 2336.
- [31] F. Pfeiffer, N. M. Felix, C. Neuber, C. K. Ober, H.-W. Schmidt, *Phys. Chem. Chem. Phys.* **2008**, *10*, 1257.
- [32] A. De Silva, C. K. Ober, *J. Mater. Chem.* **2008**, *18*, 1903.
- [33] A. De Silva, L. K. Sundberg, H. Ito, R. Sooriyakumaran, R. D. Allen, C. K. Ober, *Chem. Mater.* **2008**, *20*, 7292.
- [34] C. A. Mack, D. A. Legband, S. Jug, *Microelectron. Eng.* **1999**, *46*, 65.
- [35] L. D. Jackel, R. E. Howard, P. M. Mankiewich, H. G. Craighead, R. W. Epworth, *Appl. Phys. Lett.* **1984**, *45*, 698.
- [36] W. Hinsberg, F. A. Houle, S.-W. Lee, H. Ito, K. Kanazawa, *Macromolecules* **2005**, *38*, 1882.